ECCOMAS Congress 2016
VII European Congress on Computational Methods in Applied Sciences and Engineering
M. Papadrakakis, V. Papadopoulos, G. Stefanou, V. Plevris (eds.)
Crete Island, Greece, 5–10 June 2016

A COMPARISON OF MILP AND MINLP SOLVER PERFORMANCE ON THE EXAMPLE OF A DRINKING WATER SUPPLY SYSTEM DESIGN PROBLEM

Lea Rausch, Philipp Leise, Thorsten Ederer, Lena C. Altherr and Peter F. Pelz

Technische Universität Darmstadt, Chair of Fluid Systems
Otto-Berndt-Str. 2, 64287 Darmstadt, Germany
e-mail: {lea.rausch, thorsten.ederer, lena.altherr, peter.pelz}@fst.tu-darmstadt.de, philipp.leise@live.de

Keywords: Technical Operations Research, Mixed-Integer Nonlinear Optimisation, Solver Performance, Drinking Water Supply, System Design Problem

Abstract. *Finding a good system topology with more than a handful of components is a highly non-trivial task. The system needs to be able to fulfil all expected load cases, but at the same time the components should interact in an energy-efficient way. An example for a system design problem is the layout of the drinking water supply of a residential building. It may be reasonable to choose a design of spatially distributed pumps which are connected by pipes in at least two dimensions. This leads to a large variety of possible system topologies. To solve such problems in a reasonable time frame, the nonlinear technical characteristics must be modelled as simple as possible, while still achieving a sufficiently good representation of reality. The aim of this paper is to compare the speed and reliability of a selection of leading mathematical programming solvers on a set of varying model formulations. This gives us empirical evidence on what combinations of model formulations and solver packages are the means of choice with the current state of the art.*

1 INTRODUCTION

This paper will focus on the run-time comparison of different mathematical optimisation solvers, complementarity constraint methods and approximation methods applied to an exemplary model of the drinking water supply system in a residential building. For a more comprehensive coverage of this comparison, we vary the number of floors and the inlay pressure, whereas the overall method of modelling the pump system will remain the same. Depending on the chosen solver, complementarity constraint and approximation method, the problem will be modelled as a mixed-integer linear problem (MILP) or a mixed-integer nonlinear problem (MINLP).

Key decision for the topology problem is to find the optimal placement of pumps and pipes. Pumps can be positioned between the floors and pipes have to be laid out to connect the main water connection in the basement with the pumps and the consumers. In addition, the operational parameters for pumps are calculated, e.g. flow rate, power input and rotational speed.

To analyse the solver behaviour for different model sizes and formulations, different variations of the number of floors and the inlay pressure were created. Each combination of a number of floors and inlay pressure specifies a load setting of the pump network model. In this paper 40 different load settings were solved for all feasible combinations of solvers, constraint methods and approximation methods. This led to a total of 400 solved problems. Following solvers and methods were used and will be introduced in more detail in Section 3:

- *Solvers*: MINLP: Couenne, Scip MILP: Gurobi, GLPK
- *Complementarity Constraint Methods:* bigM (linear) and product (nonlinear) constraint
- *Approximation Methods for Characteristic Curves:*

  Linear: piecewise linear approximation by aggregated convex combination (ACC),

  Nonlinear: cubic, blending-function (Coons) and quadratic approximation

1.1 Estimation of Input Parameters

The following values, which are required to model the pump system, are calculated upfront.

1.1.1 Expected Load for Individual Floors

The minimal pressure head H_{min}, flow rate Q, and maximal flow velocity v_{max} for an individual floor are estimated by assuming a standard consumption for a flat following the European industrial standard guideline (DIN EN) [1]. The DIN EN guideline defines a standard flat with a dishwasher, kitchen sink, washbasin, shower, washing machine, and toilette. Information on the flow rates, minimal pressure, resistance coefficients, and maximal flow velocity are given. By applying the foundations of hydraulic systems [2] and assuming the hydraulic case with the highest volume flow and pressure head, the total pressure loss due to friction can be calculated. Including the minimal flow pressure from the DIN EN guideline leads to the estimated load of an individual floor given in Table1.

Parameter	Symbol	Value
minimal pressure head	H_{min}	$13\,\text{m}$
flow rate	Q	$1.50\,\text{m}^3\,\text{h}^{-1}$
maximal flow velocity	v_{max}	$2.0\,\text{m}\,\text{s}^{-1}$

Table 1: Summary of parameter estimation for individual floor.

1.1.2 Selection of Pipe Diameters

A selection rule for the pipe diameters depending on the flow rate Q is determined. The pipe diameters given in the DIN EN guideline [1] are listed in Table 2. The guideline also specifies the flow velocity v to to be within specific bounds in order to avoid microbial load and noise. We consider $0\,\text{m}^3\,\text{h}^{-1} \leq Q \leq 60\,\text{m}^3\,\text{h}^{-1}$ and $1\,\text{m}\,\text{s}^{-1} \leq v \leq 2\,\text{m}\,\text{s}^{-1}$.

Pipe diameter in mm											
10	13	16	19.6	25.6	32	39	51	60	72.1	84.9	104

Table 2: Possible diameters for pipes.

This leads to the selcetion of pipe diameters depending on the flow rate which is shown in Figure 1.

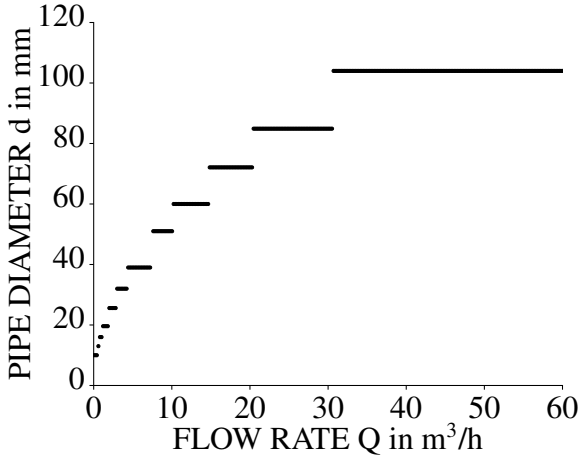

Figure 1: Pipe diameter as function depending on the flow rate.

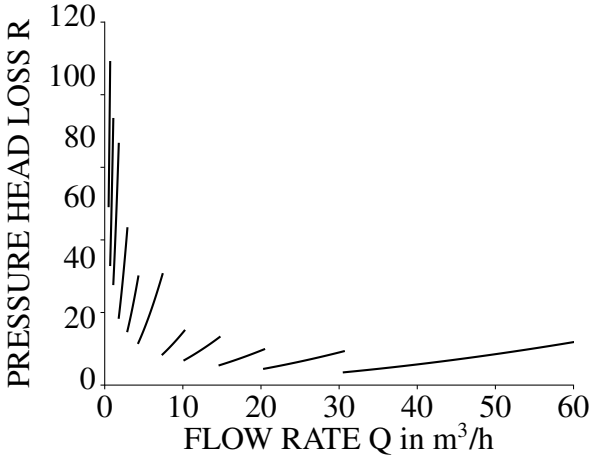

Figure 2: Linear approximation of the specific pressure head loss.

1.1.3 Approximation of Pipe Characteristics

Pressure loss due to pipe friction can be represented by the *Darcy-Weisbach* equation [2]

$$\Delta H_R = \frac{\Delta p_R}{\rho\, g} = R \cdot L = \lambda \frac{1}{2\, d_i\, g} v^2 L\,, \tag{1}$$

with pipe diameter d_i, pipe length L, gravitational constant g, average flow velocity v in pipe, friction factor λ and specific pressure loss R. Using the flow rate representation [2]

$$Q = vA = v\frac{1}{4}\pi d_i^2 \tag{2}$$

the specific pressure loss can be transformed to

$$R(Q, d_i) = \lambda \frac{1}{d_i^5}\frac{8}{\pi^2}\frac{Q^2}{g}\,. \tag{3}$$

The friction factor λ can be calculated iteratively for a fixed pipe diameter d_i and fixed flow rate Q with Newton's method. Figure 2 shows that the specific pressure loss R depends strongly on the pipe diameter and less on the volume flow. For simplification, we use the maximal specific pressure loss R_{max} for each pipe diameter as an approximation.

1.2 Pump models

In this paper, we consider three exemplary pumps from the KSB pump series Hya-Solo: EV 1/0206B, EV 1/0406B, and EV 1/0605B. The characteristics of these pumps can be found in [3]. The pump curves describe the pressure head increase and the power consumption as functions of the flow rate and rotational speed. These pump curves will be approximated with different methods which are introduced in Section 3.3.

2 MODEL

In this section, the optimisation model is presented. We do not yet focus on constraints that can be modelled in different ways: For complementarity constraints, only the formulation as disjunction is given – the explicit formulations are introduced in Section 3.2. The approximation methods of he pump characteristics are discussed in Section 3.3. The main variables and parameteres which are used in this model can be found in Table 4.

2.1 Objective Function

The model aims to minimise the sum of investment costs C of the components and the energy costs for operating the pumps:

$$\min \quad C_{\text{pipes}} + C_{\text{pumps}} + c_{\text{energy}} \cdot T \cdot P_{\text{total}}\,.$$

The operational costs c_{energy} are estimated with $0.2951\,€/\text{kWh}$ for an operating time of $T = 5$ years. The costs for the pipe purchase are estimated with $c_{\text{pipe}} = 50\,€/\text{m}$. For the pumps the investment costs are stated in the Table 3.

Pump Model	Price in €
10206/B	2344.55
10406/B	2409.35
10605/B	2484.75

Table 3: Investment costs for the different pump models.

Type	Name	Description	Value Range	Dimension
parameters	n_{floors}	number of floors		
	H_0	inlet pressure head		L
	n_{pipes}	number of possible pipes	{1,2,3,...,∞}	
	n_{pumps}	number of pumps	{3}	
	T	expected operating time of the system	[0,∞]	T
	D	ingoing and outgoing flow on each floor		L^3T^{-1}
	$h_{S\hat{S}}$	height offset between floor S and $\hat{S}$		L
	Q_{max}	maximal flow for pipe diameter	[0, 100]	L^3T^{-1}
variables	l_{pipe}	pipe length	[0,∞]	L
	P	power consumption of each pump	[0, 1800]	ML^2T^{-3}
	Q	flow rate in each pipe	[0, 100]	L^3T^{-1}
	Q_{square}	quadratic flow rate in each pipe	[0, 3600]	L^6T^{-2}
	$\hat{n}$	normalised pump rotational speed	[0.6,1]	
	ΔH	pressure head increase for each pump	[0,100]	L
	H	pressure head in each floor	[0,100]	L
	k_{pipe}	indicator for pipe selection	{0,1}	
	k_{pump}	indicator for pump placement on a pipe	{0,1}	
	R_{pipe}	specific pressure loss due to pipe friction	[0,∞]	
	d_{pipe}	selected pipe diameter	[9,105]	L
	k_{Q}	non-zero flow indicator	{0,1}	

Table 4: Main input parameters and decision variables of the optimisation model.

Expressed in decision variables, the objective is

$$\begin{aligned} \min \quad & \sum_{i=1}^{n_{\text{pipes}}} \sum_{j=1}^{n_{\text{pumps}}} k_{\text{pump}}(i,j) \cdot c_{\text{pump}}(j) \\ & + \sum_{i=1}^{n_{\text{pipes}}} k_{\text{pipe}}(i) \cdot c_{\text{pipe}} \cdot l_{\text{pipe}}(i) \\ & + c_{\text{energy}} \cdot T \cdot \sum_{i=1}^{n_{\text{pipes}}} \sum_{j=1}^{n_{\text{pumps}}} P(i,j)\,. \end{aligned} \tag{4}$$

2.2 Constraints

Pipe indicators model the interconnection of floors. The correspondence of pipes and floors can be encoded by a matrix A where a_{ij} is equal to the index $k \in \{1, ..., n_{\text{pipes}}\}$ of the pipe which connects floor i with floor j. Pipes can only be placed from a lower floor to one above, i.e. $a_{ij} = 0\ \forall j \leq i$. Hence, the number of pipes in the model is given by $n_{\text{pipes}} = \frac{1}{2} n_{\text{floors}}(n_{\text{floors}} - 1)$. Only one pipe can be chosen to reach one floor:

$$\sum_{i=1}^{n_{\text{floors}}} k_{\text{pipe}}(a_{ij}) \leq 1, \qquad \forall j \in \{2, ..., n_{\text{floors}}\}\,. \tag{5}$$

In addition, a bigM or product constraint for the following complementarity expression (c.f. Section 3.2) is required to allow a flow rate only if the pipe is selected:

$$expr = Q(k,j) \text{ depending on } k_{\text{pipe}}(k) \qquad \forall\, k \in \{1,2,...,n_{\text{pipes}}\}\,. \tag{6}$$

The pipe diameters need to be selected as described in Section 1.1.2. Let the parameters $d_{\text{values}}(i)$ be the possible pipe diameters and $Q_{jd}(i)$ the flow rates at the jump discontinuities in Figure 1.

$$\begin{aligned} Q(j) &\le Q_{\text{max}} && \forall j \in \{1,2,...,n_{\text{pipes}}\}\,, \\ Q(j) &\ge Q_{jd}(i)\cdot k_{\text{Q}}(j,i) && \forall j \in \{1,2,...,n_{\text{pipes}}\}\,, \\ & && \forall i \in \{1,2,...,12\} \\ Q(j) &\le Q_{jd}(i+1)\cdot k_{\text{Q}}(j,i) + Q_{\text{max}}\cdot(1-k_{\text{Q}}(j,i)) && \forall j \in \{1,2,...,n_{\text{pipes}}\}\,, \\ & && \forall i \in \{1,2,...,12\}\,, \\ d_{\text{pipe}} &= \sum_{i=1}^{12} k_{\text{Q}}(j,i)\cdot d_{\text{values}}(i) && \forall j \in \{1,2,...,n_{\text{pipes}}\}\,. \end{aligned} \tag{7}$$

To model the flow requirements, let I be the $(n_{\text{pipes}} \times m)$ incidence matrix and D the input (positive value) and output (negative value) flows of the floors. The continuity equation [4] on networks can be implemented by the following constraints:

$$\sum_{k=1}^{m} I(i,k)\, Q(k) = D(i) \qquad \forall i \in \{1,...,n_{\text{pipes}}\}\,. \tag{8}$$

The pipe friction is included based on the estimation in Section 1.1.3 and can be modelled by a bigM or product constraint for the following complementarity expression which is active in a pipe if the flow rate is higher than 0, i.e., if $k_{\text{Q}}(i,k) = 1$:

$$\begin{aligned} expr = R(i) - R_{\text{max}}(k) \quad &\text{depending on } k_{\text{Q}}(i,k) \quad \forall\, i \in \{1,2,...,n_{\text{pipes}}\}, \\ & \qquad\qquad\qquad\quad \forall\, k \in \{2,...,12\}\,. \end{aligned} \tag{9}$$

The pressure requirement for each floor from Table 1 gives the minimal pressure head H_{min}:

$$\begin{aligned} H(1) &= H_0 && , \\ H(k) &\ge H_{\text{min}} && \forall\, k \in \{2,...,n_{\text{floors}}\}\,. \end{aligned} \tag{10}$$

In addition, a bigM or product constraint for the following complementarity expression is required to model the differences of the pressure head between the floors S and $\hat{S}$ for each selected pipe:

$$\begin{aligned} expr = H(\hat{S}) - \Delta H(i,1) - \Delta H(i,2) - \Delta H(i,3) + h_{S\hat{S}} + R(i)\cdot h_{S\hat{S}} - H(S) \\ \text{depending on } k_{\text{pipe}}(k) \qquad \forall\, k \in \{1,2,...,n_{\text{pipes}}\}\,. \end{aligned} \tag{11}$$

The network dependencies are given by:

$$\begin{aligned} k_{\text{pump}}(k,i) &\le k_{\text{pipe}}(k) && \forall\, i \in \{1,2,3\}\,, \\ & && \forall\, k \in \{1,2,...,n_{\text{pipes}}\}\,. \end{aligned} \tag{12}$$

To include the relationship of flow rate Q, rotational speed $\hat{n}$, power P and pressure head ΔH as given by the pump curves, the general constraints are shown here. The exact formulas for $\tilde{P}$

and $\tilde{H}$ depend on the selected approximation method of the pump curves which are described in Section 3.3:

$$P(i,j) = k_{\text{pump}}(i,j) \cdot \tilde{P}(Q(i), \hat{n}(i,j)) \qquad \begin{array}{l} \forall\, i \in \{1,..,n_{\text{pipes}}\}\,, \\ \forall\, j \in \{1,..,n_{\text{pumps}}\}\,, \end{array} \tag{13}$$

$$\Delta H(i,j) = k_{\text{pump}}(i,j) \cdot \tilde{H}(Q(i), \hat{n}(i,j)) \qquad \begin{array}{l} \forall\, i \in \{1,..,n_{\text{pipes}}\}\,, \\ \forall\, j \in \{1,..,n_{\text{pumps}}\}\,. \end{array} \tag{14}$$

In addition, the variables Q and $\hat{n}$ need to be restricted to the value range which is included in the pump curves.

3 SELECTED SOLVERS AND METHODS

This section gives a short introduction of all compared solvers, constraint methods and approximation methods including a quality analysis of the approximation methods.

3.1 Solvers

The presented comparison includes four different solvers. Two solvers, Gurobi and GLPK, for linear problems and two for nonlinear problems, Couenne and Scip. Except of Gurobi all solvers are open source. A short general description of the used solver can be found below. *Gurobi* is a commercial solver for mixed-integer linear problems (MILP), as well as linear problems (LP). A new version of Gurobi can also include quadratic aspects but is not used in this paper. The solver is provided by the company Gurobi [5]. *GLPK* (GNU Linear Programming Kit) includes an open source solver for mixed-integer linear problems (MILP), as well as linear problems (LP). GLPK works with the GNU MathProg modelling language, which is a supported by the Free Software Foundation [6]. *Couenne* (Convex Over and Under ENvelopes for Nonlinear Estimation) is an open source solver for mixed-integer nonlinear problems (MINLP). The solver is provided by the Computational Infrastructure For Operations Research Foundation (COIN-OR) [7]. *Scip* (Solving Constraint Integer Programs) is a commercial open source solver for mixed-integer nonlinear problems (MINLP) as well as for mixed-integer linear problems (MILP). Scip is directed towards meeting the needs of Mathematical Programming experts who are interested in a high level of control and detailed information of the solution process. The solver is provided by the Zuse Institute Berlin (ZIB) [8].

3.2 Methods to Model Complementarity Constraints

In general, complementarity constraints describe the following relation:

$$expr_1 = 0 \;\vee\; expr_2 = 0\,. \tag{15}$$

We will compare two different methods to model complementarity constraints, which are used to activate and deactivate equality constraints depending on the value of an auxiliary decision variable. The linear bigM method and the nonlinear product method. As the product complementarity constraint is nonlinear, it can not be used with the linear solvers Gurobi and GLPK.

For both methods assume $expr = 0$ is a linear constraint for a number of decision variables which only needs to be met if the auxiliary binary decision variable $k \in \{0,1\}$ is active, i.e. $k = 0$. This requirement can be modelled with the following constraints.

3.2.1 bigM Method

Let $bigM \in \mathbb{R}^+$ be a sufficiently big positive constant. Then the above described requirement can be modelled with the constraint (16).

$$\begin{aligned} expr &\leq +\, k \text{ bigM}\,, \\ expr &\geq -\, k \text{ bigM}\,. \end{aligned} \tag{16}$$

The choice of $bigM$ needs to guarantee $-\text{bigM} \leq expr \leq \text{bigM}$ for any feasible combinations of the decision variables in $expr$. Nevertheless, $bigM$ should be estimated as small as possible, as a big value for $bigM$ increases the risk of numerical errors.

3.2.2 Product Method

To reduce numerical errors caused by the bigM method, one can use the standard complementarity constraint in product form (17) for nonlinear solvers instead.

$$(expr)\,(1-k) = 0\,. \tag{17}$$

3.3 Approximation Method

Pump curves are used to represent the key pump characteristics and show the pressure head increase $\Delta H(\hat{n}, Q)$ as a function over the rotational speed and flow rate as well as the required power input $P(\hat{n}, Q)$. These pump curves need to be approximated for the MI(N)LPs. For this comparison one linear and three nonlinear approximation methods are used and the quality of all four methods is analysed by validating the affinity laws, c.f. Section 3.3.5.

3.3.1 Piecewise Linearization by Aggregated Convex Combination

An aggregated convex combination formulation based on a Freudenthal triangulation [9] is used as piecewise linear approximation method. The surfaces which describe the pump curves $\Delta H(\hat{n}, Q)$ and $P(\hat{n}, Q)$ are cut into triangles. In each triangle the curve is approximated by a linear triangle spanned by the grid points of the pump curve. Hence, in each grid point the approximation equals the actual pump curve. In every other point, the approximation is a linear combination of the three surrounding grid points. In this paper a 7x7 triangulation is used which leads to 49 grid points.

3.3.2 Cubic Approximation

For the cubic method the pump curves are approximated with the cubic functions (18) where the coefficients $a, b, c, \alpha, \beta, \gamma$ and δ are determined by a regression analysis. In the regression analysis the rotational speed is scaled to the maximal pump rotational speed n_{ref}, i.e. $\hat{n} = \frac{n}{n_{\text{ref}}}$.

$$\begin{aligned} \Delta H(\hat{n}, Q) &= aQ^2 + bQ\hat{n} + c\hat{n}^2\,, \\ P(\hat{n}, Q) &= \alpha Q^3 + \beta Q^2\hat{n} + \gamma Q\hat{n}^2 + \delta\hat{n}^3\,. \end{aligned} \tag{18}$$

The results of the regression analysis for the three different pump models pumps Hya-Solo EV 1/0206B, Hya-Solo EV 1/0406B and Hya-Solo EV 1/0605B are shown in Table 5 for the pressure head increase ΔH and for the power consumption P. In this table one can also find the

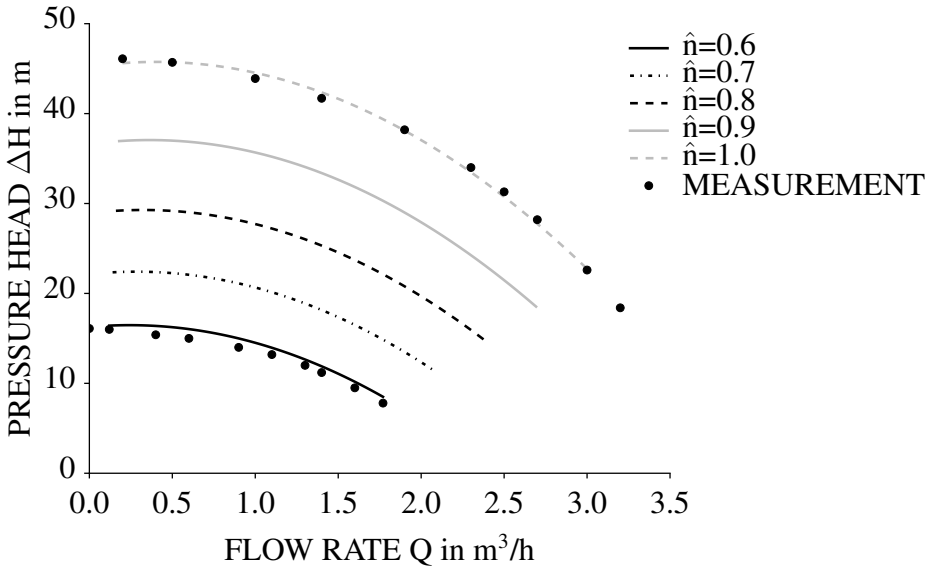

Figure 3: Cubic approximation of pressure head increase in pump curve for the pump model Hya-Solo EV 1/0206B.

standard error $\epsilon_\beta(j)$ for each coefficient of the approximation which is calculated with the MSE (*mean squares of errors*) $\sigma_r^2 = \frac{\sum_{i=1}^{m} \epsilon^2}{m-p-1}$ leading to the standard error $\epsilon_\beta(j) = \sigma_r \sqrt{(X^T X)^{-1}_{jj}}$, c.f. [10].

Figure 3 shows the cubic approximation of the pump curve for the pressure increase $\Delta H(\hat{n}, Q)$.

3.3.3 Bending-Function (Coons) Approximation

The Coons approximation method [11] is not physically motivated but based on graphical data processing. It interpolates the pump curve with an auxiliary variable s with $0 \leq s \leq 1$. The pump curve is approximated as a linear function of s and a quadratic function of the second variable Q:

$$\begin{aligned} \Delta H(s, Q) &= (a_1 Q^2 + b_1 Q + c_1)s + (a_2 Q^2 + b_2 Q + c_2)(1 - s)\,, \\ P(s, Q) &= (\alpha_1 Q^2 + \beta_1 Q + \gamma_1)s + (\alpha_2 Q^2 + \beta_2 Q + \gamma_2)(1 - s)\,. \end{aligned} \tag{19}$$

For all pump models the results of the regression analysis can be found in the appendix in Table 7 and 8.

3.3.4 Quadratic Approximation

A further nonlinear approximation method is a complete quadratic approximation [12] for $0.6 \leq \hat{n} \leq 1$. This approximation is *not* physically motivated and does not adhere to the affinity laws. However, due to its lower polynomial degree, it might speed up the computation without too much of a deviation from the cubic approximation.

$$\begin{aligned} \Delta H(\hat{n}, Q) &= aQ^2 + bQ\hat{n} + c\hat{n}^2\,, \\ P(\hat{n}, Q) &= \alpha Q^2 + \beta\hat{n}^2 + \gamma Q\hat{n} + \delta Q + \epsilon\hat{n} + \zeta\,. \end{aligned} \tag{20}$$

The approximation for the pressure head increase is the same as for the cubic approximation 3.3.2. Therefore, the coefficients a, b and c can be taken from the cubic regression analysis in

Coefficient	Value	Error
a_{206}	-3.415	0.25
b_{206}	2.760	0.87
c_{206}	45.193	0.63
a_{406}	-0.921	0.085
b_{406}	1.177	0.55
c_{406}	52.296	0.75
a_{605}	-0.345	0.04
b_{605}	0.373	0.35
c_{605}	47.973	0.65

Coefficient	Value	Error
α_{206}	-11.142	2.52
β_{206}	41.522	13.29
γ_{206}	54.318	19.61
δ_{206}	191.211	7.75
α_{406}	-1.774	0.79
β_{406}	5.902	7.59
γ_{406}	135.815	19.57
δ_{406}	245.276	12.86
α_{605}	-0.664	0.12
β_{605}	1.154	1.59
γ_{605}	125.728	5.84
δ_{605}	276.781	5.81

Table 5: Coefficients for the cubic approximation of the pressure head ΔH (right) and the power consumption P (left) for each of the three pump models 10**206**/B, 10**406**/B, 10**605**/B. The coefficients of the other approximation methods can be found in the appendix.

Table 5. The coefficients α, β, γ, δ, ϵ and ζ need to be determined in an additional regression analysis. The results for the power consumption P for the three different pump models can be found in the appendix in Table 9.

3.3.5 Quality Analysis of Approximation Methods

For comparison, four approximation methods are applied. We want to analyse how well they match reality. The functional correlation of pump rotational speed $\hat{n}$, flow rate Q and pressure head ΔH are described by affinity laws [13]. They imply the following proportionality:

$$Q \sim \hat{n}, \quad \Delta H \sim \hat{n}^2, \quad \text{and} \quad P \sim \hat{n}^3 \,. \tag{21}$$

These proportionality relations can be transformed to the following quality measure (22) for the approximation methods. The error value E indicates the adherence to the affinity law and therefore the fit quality of the approximation method:

$$E_Q = \frac{Q_1}{Q_2} - \frac{\hat{n}_1}{\hat{n}_2} \approx 0, \quad E_H = \frac{\Delta H_1}{\Delta H_2} - \left(\frac{\hat{n}_1}{\hat{n}_2}\right)^2 \approx 0 \text{ and } E_P = \frac{P_1}{P_2} - \left(\frac{\hat{n}_1}{\hat{n}_2}\right)^3 \approx 0 \,. \tag{22}$$

To measure the quality of the approximation method, a set of 1000 grid points were inserted in the approximation of the pump curve and the results used to calculate the errors in (22). The results are listed in Table 6 in the appendix. The error analysis shows that all used approximation methods have a similar and low error level. The only exception is the bending-function (Coons) approximation method which causes a higher average error for the pressure head E_H for all tested pump models.

4 OPTIMISATION RESULTS FOR A SELECTED EXAMPLE

In most cases, the topology results of different solver and method combinations for one load setting are the same or vary only slightly, c.f. Section 5.4.

We chose an example with a residential building with three floors. In the optimised topology in Figure 4 one pump of type Hya-Solo EV 1/0206B is used between the second and third floor.

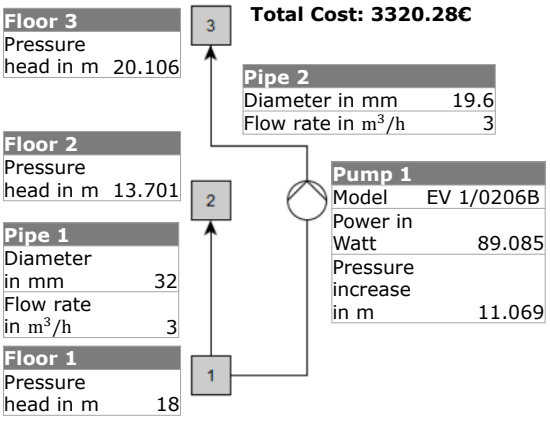

Figure 4: Example of optimal topology with 16% savings compared to standard approach.

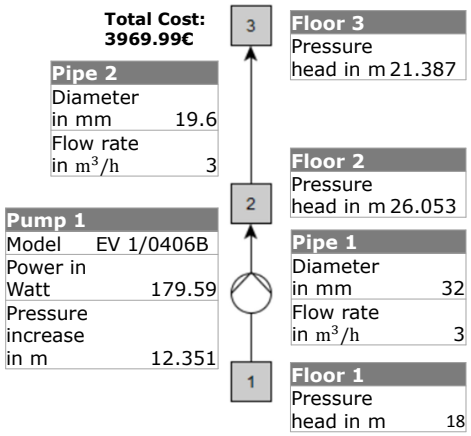

Figure 5: Example topology with pumps only on the first floor.

Compared to the basic approach to place all pumps in the first floor, the optimal solution for this example reduces the sum of investment costs of the components and energy costs for operating the pumps by 16%. Following the basic approach it is necessary to use the more expensive pump Hya-Solo EV 1/0406B to gain the relevant flow rate and pressure head from the pump in the first floor to the third floor, see Figure 5.

5 EMPIRICAL RESULTS

All methods show the expected result of the commercial solver Gurobi excelling clearly in run-time performance, especially for a growing model size.

When comparing the geometric mean of run-times over all problems for the best method per solver, it is necessary to focus on lower number of floors, e.g. 7 or 8 floors. The reason is that the problems with a high number of floors could not be solved to optimality with all solvers and all methods within the time limit of six hours (details see Section 5.2).

For 7 floors the best method combination for Counne and Scip is far closer to Gurobi than for the geometric mean over all methods. This shows the relevance of the right method choice: Scip takes about 9 times the geometric mean time of Gurobi over all problems. When comparing the best suitable method combination for Scip (bigM constraints and quadratic pump curve approximation), it takes only 4 times the geometric mean time of Gurobi. For Counne the difference of the geometric mean run times to Gurobi drops from factor 135 to 28 for the best suitable combination (product complementarity constraints with quadratic approximation).

5.1 Number of Constraints and Variables

For all pump characteristic approximations and complementarity constraint methods, the number of constraints as well as the number of variables grow quadratically in the number of floors. The linear approximation has by far the highest numbers with around 4,500 constraints and 8,300 variables for 7 floors compared to the nonlinear approximation methods which all have about 1,500 constraints and 1,000 variables. For 10 floors the linear approach leads to 9,700 constraints and 18,000 variables, whereas the nonlinear methods have 2,500 constraints and 1,600 variables.

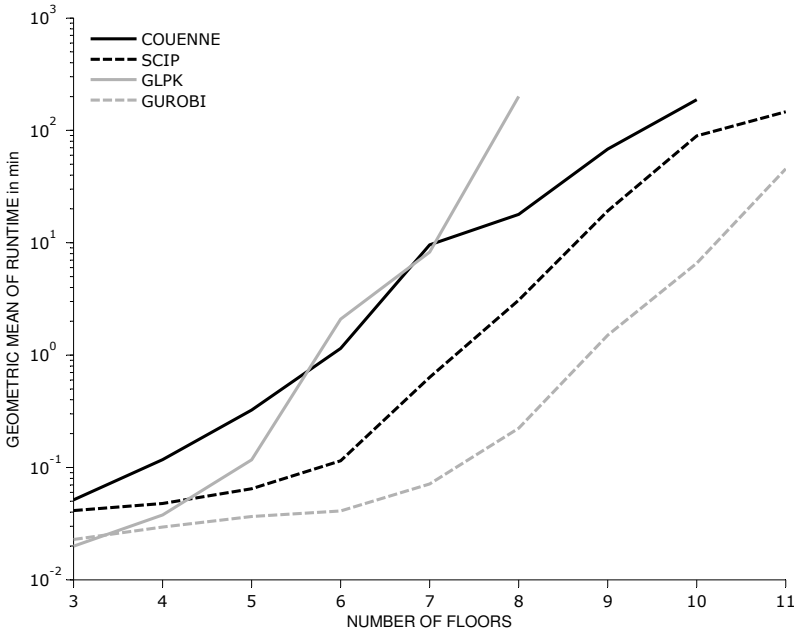

Figure 6: All solvers with geometric mean of run-times over all approximation and constraint methods as well as all inlet pressures for each number of floors.

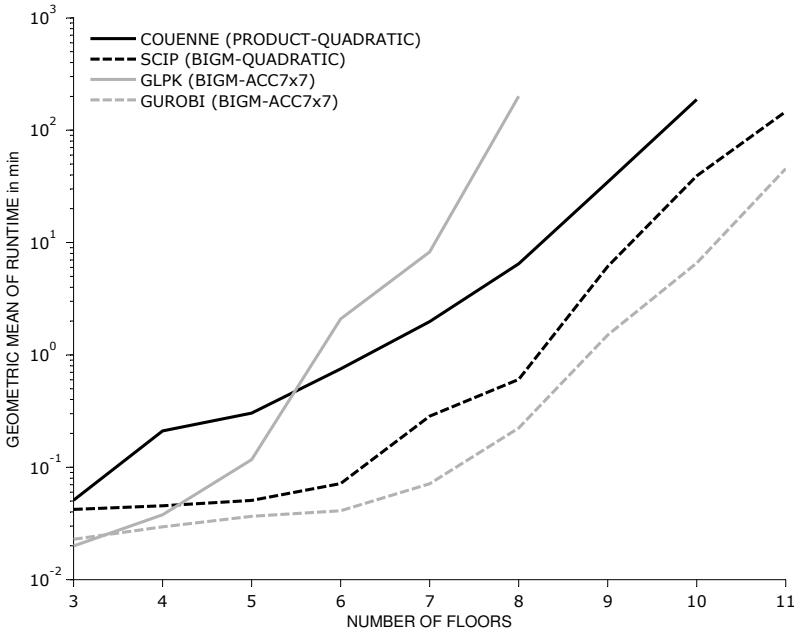

Figure 7: All solvers with geometric mean over all problems solved with the best combination of methods for teach solver over all inlet pressures for each number of floors.

5.2 Method Analysis for Individual Solvers

For the nonlinear solvers, we used a total of six different combinations of pump characteristic approximations and complementarity constraint methods. In this section, we show how they influence the run-time of the individual solvers.

5.2.1 Couenne

The highest influence on the run-time of the Couennne solver is caused by the method to model the complementarity constraints, as each approximation method combined with the bigM method has a higher run-time than any approximation method combined with the product method for complementarity constraints. There is also a strong increase of the differences in run-time between the complementary methods starting with seven floors.

Comparing the approximation methods one can see that for bigM complementarity constraints the cubic approximation methods outperforms the quadratic approximation, whereas for complementarity constraints it is the other way around and the quadratic approximation outperforms the cubic approximation, especially for a high number of floors. Even though Coons is a simplification of the cubic equations, it has the highest run time for both complementary methods for a high number of floors; for the product method starting with 7 floors, for bigM starting with 5 floors.

5.2.2 Scip

Contrary to Couenne, for the Scip solver the approximation method for the pump curves has the highest influence on run time. This is shown as every method to model the complementarity constraints combined with the Coons approximation is worse than every complementarity constraints method combined with the other two approximation methods.

Comparing the two other approximation methods, one can see that for bigM complementarity constraints the quadratic approximation method outperforms the cubic approximation. Whereas, for product complementarity constraints it is the other way around, especially for a high number of floors. BigM is the better complementarity constraint method for Scip since for each approximation method the bigM method has a shorter geometric mean run-time than the same approximation method combined with product complementarity constraints.

5.3 Comparison of Scip and Couenne

In Figure 5 one can see that Scip with its best combination (bigM complementarity constraint and quadratic approximation) outperforms compared to Couenne's best combination (product complementarity constraint and quadratic approximation), as well as in the overall comparison with the geometric mean run-time of all combinations.

As already discussed in the individual solver analysis, the product complementarity constraint methods works better for Couenne as for Scip. In Figure 5.4 one can see that for 10 floors this difference is so severe that the in average slower solver Couenne outperforms Scip when using the product complementarity constraint method.

5.4 Objective Values and Boundaries of the Presented Methods

In most cases, all solvers, approximation methods and constraint types result in similar topology decisions for the same load setting with only a small deviation in the objective function value due to numerical differences. Only for 4% of all solved problems the objective value deviates more than 5% (but no more than 26%) from the average objective value of all problems belonging to this load setting. In these cases, a small deviation of the topology is possible.

An exception with a different topology decision and objective value deviation of 88% occurs when using the solver Scip with cubic approximation method for one load setting with a high inlet pressure ($H_0 = 17\,\mathrm{m}$) with a low number of floors ($n_{\text{floors}} = 3$). For this load setting,

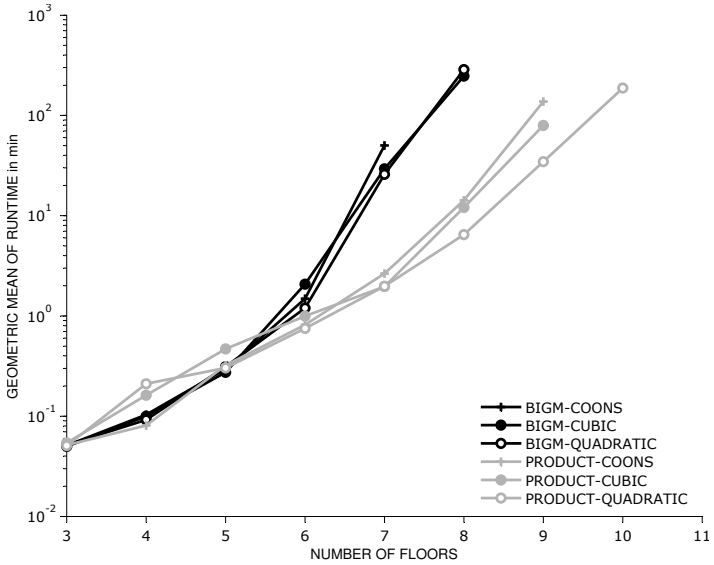

Figure 8: Couenne solver with geometric mean of run-times over all inlet pressures for each number of floors for each combination of approximation and complementary methods.

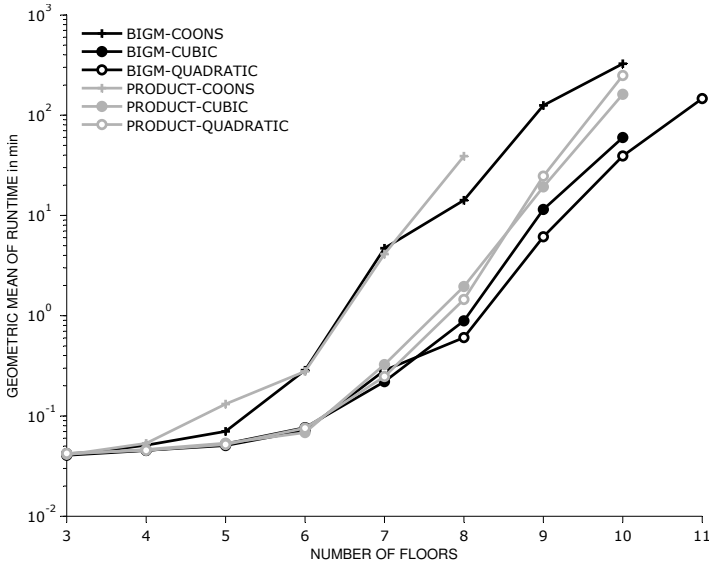

Figure 9: Solver Scip with geometric mean of run-times over all inlet pressures for each number of floors for each combination of approximation and complementary methods.

the topological solution using Scip with cubic approximation method with bigM as well as with product complementarity constraint method differs strongly from all other solutions of the same load setting. With the cubic approximation method no pump is selected in the whole system whereas one pump is selected in all other solutions of this load setting. We assume it is caused by the high numerical complexity of the cubic approximation method, as the inlet pressure is relatively high for the number of floors. This hypothesis is supported by the solutions for a different load setting with an even higher inlet pressure of ($H_0 = 23\,\mathrm{m}$) with the same number of floors ($n_{\text{floors}} = 3$). For this second load setting, all solutions (with all combinations of solvers, constraint and approximation method) contain the topology decision to use no pump, as the inlet pressure is sufficient to supply all floors.

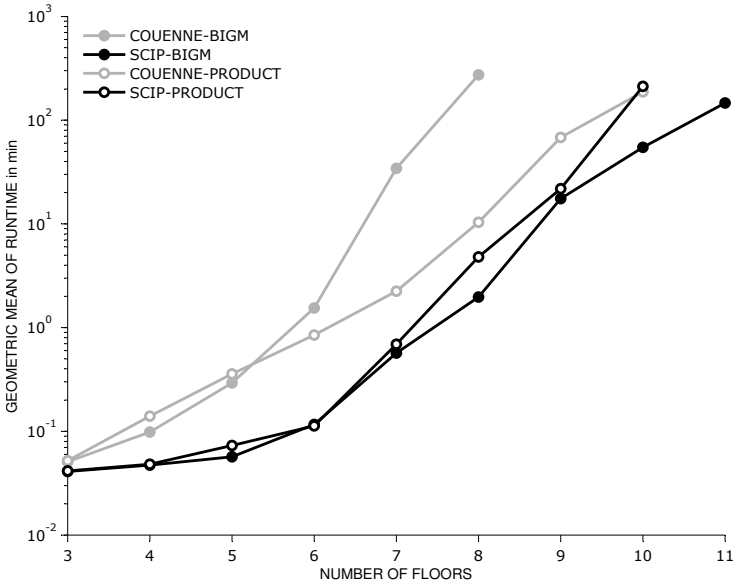

Figure 10: Geometric mean of run time over all inlet pressures and all approximation methods for each number of floors for each complementary method for Couenne and Scip.

6 CONCLUSIONS

- A model to design spacially distributed fluid systems has been developed and verified.
- Savings of energy and investment costs by applying the developed model could be detected for an example load setting.
- Solver runtime was compared depending on various combinations of solvers, complementarity constraint methods and approximation methods for pump characteristics.
- Optimal solutions from different solvers and methods vary only slightly, but the run-times deviate severely.
- Approximation methods with simpler equations can lead to higher run-times.

7 ACKNOWLEDGEMENT

This work is partially supported by the German Federal Ministry for Economic Affairs and Energy funded project ‘Entwicklung hocheffizienter Pumpensysteme’ and by the German Research Foundation (DFG) funded Collaborative Research Centre SFB 805.

8 APPENDIX

Pump Model	Approximation	Error Type	Average	Standard Deviation
EV 1/0206B	cubic	E_Q	-7.11×10^{-19}	3.74×10^{-33}
		E_H	-4.27×10^{-18}	1.36×10^{-16}
		E_P	-3.69×10^{-19}	1.52×10^{-32}
	coons	E_Q	5.55×10^{-19}	3.79×10^{-33}
		E_H	-3.50×10^{-2}	6.94×10^{-3}
		E_P	-1.83×10^{-2}	3.76×10^{-3}
	quadratic	E_Q	-9.44×10^{-19}	3.61×10^{-33}
		E_H	-4.35×10^{-18}	1.40×10^{-16}
		E_P	6.26×10^{-4}	4.35×10^{-5}
	linear	E_Q	4.00×10^{-19}	3.70×10^{-33}
		E_H	-1.16×10^{-3}	3.12×10^{-3}
		E_P	-3.54×10^{-4}	1.29×10^{-5}
EV 1/0406B	cubic	E_Q	-3.33×10^{-20}	3.70×10^{-33}
		E_H	-8.30×10^{-18}	1.40×10^{-16}
		E_P	1.72×10^{-19}	1.56×10^{-32}
	coons	E_Q	-8.55×10^{-19}	3.52×10^{-33}
		E_H	2.60×10^{-1}	1.95×10^{-1}
		E_P	2.24×10^{-1}	1.22×10^{-1}
	quadratic	E_Q	6.66×10^{-19}	3.78×10^{-33}
		E_H	-9.92×10^{-18}	1.38×10^{-16}
		E_P	-2.22×10^{-4}	2.66×10^{-6}
	linear	E_Q	-4.33×10^{-19}	3.70×10^{-33}
		E_H	-1.45×10^{-3}	3.96×10^{-3}
		E_P	-1.42×10^{-3}	2.78×10^{-5}
EV 1/0605B	cubic	E_Q	5.55×10^{-19}	3.91×10^{-33}
		E_H	-5.42×10^{-18}	1.34×10^{-16}
		E_P	2.03×10^{-18}	1.66×10^{-32}
	coons	E_Q	-5.33×10^{-19}	3.49×10^{-33}
		E_H	2.61×10^{-1}	1.78×10^{-1}
		E_P	2.38×10^{-1}	1.40×10^{-1}
	quadratic	E_Q	-3.00×10^{-19}	3.86×10^{-33}
		E_H	-5.91×10^{-18}	1.34×10^{-16}
		E_P	-1.75×10^{-4}	6.67×10^{-5}
	linear	E_Q	6.88×10^{-19}	4.05×10^{-33}
		E_H	9.33×10^{-4}	2.57×10^{-3}
		E_P	-1.51×10^{-3}	2.42×10^{-5}

Table 6: Error in affinity laws for the pump characteristic approximation methods.

Coefficient	Value	Error
$a_{206}(1)$	-3.415	0.25
$a_{206}(2)$	-2.761	0.23
$b_{206}(1)$	2.760	0.87
$b_{206}(2)$	0.397	0.42
$c_{206}(1)$	45.193	0.63
$c_{206}(2)$	15.940	0.15
$a_{406}(1)$	-0.921	0.08
$a_{406}(2)$	-0.902	0.08
$b_{406}(1)$	1.177	0.55
$b_{406}(2)$	0.601	0.32
$c_{406}(1)$	52.296	0.75
$c_{406}(2)$	17.991	0.25
$a_{605}(1)$	-0.345	0.04
$a_{605}(2)$	-0.329	0.03
$b_{605}(1)$	0.373	0.35
$b_{605}(2)$	0.129	0.14
$c_{605}(1)$	47.973	0.65
$c_{605}(2)$	16.257	0.15

Table 7: Coefficients for the bending-function (Coons) approximation of the pressure head characteristic for each of the three pump models 10**206**/B, 10**406**/B, 10**605**/B.

Coefficient	Value	Error
$\alpha_{206}(1)$	-16.441	3.97
$\alpha_{206}(2)$	-14.684	3.23
$\beta_{206}(1)$	134.804	14.42
$\beta_{206}(2)$	51.325	6.34
$\gamma_{206}(1)$	165.890	10.51
$\gamma_{206}(2)$	39.560	2.38
$\alpha_{406}(1)$	-10.958	1.68
$\alpha_{406}(2)$	-3.328	2.42
$\beta_{406}(1)$	175.426	11.20
$\beta_{406}(2)$	44.981	10.05
$\gamma_{406}(1)$	231.090	14.55
$\gamma_{406}(2)$	72.840	9.05
$\alpha_{606}(1)$	-7.667	0.78
$\alpha_{605}(2)$	-3.125	1.34
$\beta_{605}(1)$	154.842	7.27
$\beta_{605}(2)$	42.054	6.96
$\gamma_{605}(1)$	260.489	13.48
$\gamma_{605}(2)$	72.679	7.40

Table 8: Coefficients for the bending-function (Coons) approximation of the power characteristic for each of the three pump models 10**206**/B, 10**406**/B, 10**605**/B.

Coefficient	Value	Error
α_{206}	-10.509	0.09
β_{206}	554.656	0.34
γ_{206}	177.974	0.62
δ_{206}	-57.797	0.46
ϵ_{206}	-552.849	5.40
ζ_{206}	169.975	2.13
α_{406}	-9.462	0.03
β_{406}	888.804	4.60
γ_{406}	241.806	0.45
δ_{406}	-72.719	0.33
ϵ_{406}	-963.466	7.29
ζ_{406}	304.907	2.89
α_{605}	-6.729	0.02
β_{605}	1034.160	5.54
γ_{605}	208.700	0.38
δ_{605}	-60.132	0.28
ϵ_{605}	-1125.230	8.73
ζ_{605}	354.673	3.43

Table 9: Coefficients for quadratic approximation of power characteristic for each of the three pump models 10**206**/B, 10**406**/B, 10**605**/B. The coefficients for the pressure head characteristic are given by the cubic coefficients in Table 5 (left).

REFERENCES

[1] DIN EN 806-3:2006-07 (and underlying DIN 1988-300):2012-05, *Technische Regeln f¨r Trinkwasser-Installationen - Teil 3: Berechnung der Rohrinnendruchmesser - Vereinfachte Verfahren.* Beuth Verlag, 2006.

[2] H. Martin, R. Pohl, *Technische Hydromechanik 4: Hydraulische und numerische Modelle.* Beuth Verlag, 2015.

[3] KSB Aktiengesellschaft, *Baureihenheft hya-solo*, https://shop.ksb.com/ims_docs/00/005056B602221ED4A9CD0BF2DE4AAB88.pdf, 04.09.2015 17:55.

[4] D. Aigner, D. Carstensen. *Technische Hydromechanik 2: Spezialfälle.* Volume 2, Beuth Verlag, 2013.

[5] Gurobi *Website Gurobi Optimiser.* http://www.gurobi.com/products/gurobi-optimizer 10.02.2016 09:10

[6] GNU *Website GLPK* https://www.gnu.org/software/glpk/ 10.02.2016 09:10

[7] Coin OR *Website.* http://www.coin-or.org/Couenne/ 10.02.2016 08:50

[8] Zuse Institue Berlin *Website SCIP* http://scip.zib.de/ 10.02.2016 09:10

[9] K. Weiss, L. De Floriani, *Simplex and diamond hierarchies: Models and applications.* Computer Graphics Forum, volume 30, pages 21272155, Wiley Online Library, 2011.

[10] S. Chatterjee, J. S. Simonoff. *Handbook of Regression Analysis* John Wiley & Sons, Inc, 2013.

[11] R. Forrest *On coons and other methods for the representation of curved surfaces.* Computer Graphics and Image Processing, 1(4):341359, 1972.

[12] I.N. Bronstein, K.A. Semendjajew, G. Musiol, H Mhlig. *Taschenbuch der Mathematik* 7. vollstndig berarbeitete und ergnzte Auflage. Verlag Harri Deutsch, 2008.

[13] G.K. M. Pedersen, Z. Yang. *Efficiency optimization of a multi-pump booster system.* Proceedings of the 10th annual conference on Genetic and evolutionary computation, pages 16111618. ACM, 2008.